International Journal of Robotics and Mechatronics

Thermal Imaging-Based Human Emotion Detection: GLCM Feature Extraction Approach

M.H. Abd Latif, Md. Yusof Hazlina, and S.N. Sidek

Department of Mechatronics Engineering, International Islamic University Malaysia, Kuala Lumpur, Malaysia

***Abstract*—**Recent studies in artificial intelligence and robotics had proved the ability of social intelligence in robots. However, it has become increasingly apparent that social and interactive skills are necessary requirements in any application areas and contexts where robots need to interact and collaborate with other robots or humans. In order to develop an emotionally intelligent robot, the issues on how to perceive human affective states and how to manifest the robot's emotion should be addressed. In this paper, we presented an efficient method for thermal image feature extraction using the Gray Level Co-occurrence Matrix (GLCM) technique. By analysing the heat pattern on the facial skin, this work attempt to investigate the suitability of the thermal imaging technique for affect detection. The findings of this study indicate thermal imaging as an alternative, contactless and noninvasive method for appraising human emotional states.

***Keywords*—**Affect detection, human robot interaction, thermal image, Gray Level Co-occurrence Matric (GLCM).

I. Introduction

PICARD [1] states that "Emotion plays an essential role in rational decision-making, perception, learning and a variety of functions". Emotional reactions are categorized as a set of responses to internal and external occurrences which involve shared contribution of behavioral, cognitive, physiological and neural mechanism to orchestrated desirable responses [2]. In social interaction, explicit and implicit communication plays a significant role in an effective interaction. Nonetheless, meaningful communication sometimes could not be achieved as the typical modalities of interaction (verbal and body language) might be deterred when dealing with an individual with special needs; Autistic, Asperger, ADHD, etc. [3]. In order to provide an effective engagement with the emotionally-challenged subject, apprehension of their emotional states is highly intrinsic. For decades, issues related to affects importance in the development of autonomous system have been addressed yet little effort has been taken in assimilating affects into the intelligent system. For robotics systems being part of the society, the robots should have the ability to perceive the operator's affective states in response to the robots' actions. A robotic system that has the capability of recognising emotional states and synthesising proper responses would be beneficial for Human-Robot Interaction (HRI). Hence, empowering computers and robots to understand human emotions would make human-robot interaction more meaningful. The potential applications of robots that could detect a person's affective state and respond accordingly to such perceptions are diverse (personal home aids, entertainment robot, rescue and surveillance robots etc.). Recent studies in artificial intelligence and robotics have proven the ability of social intelligence in robots. Over the years, the trend in emotionally and socially aware system research has been escalating which demonstrates the importance of HRI.

Corresponding author: Md. Y. Hazlina (e-mail: myhazlina@iium.edu.my).
This paper was submitted on December 4, 2015; revised on December 20, 2015; and accepted on December 27, 2015.

The emotion recognition could be achieved through an affective computing method to compute the human emotions. Over a decade, there have been rigorous researches on robots as tools for rehabilitation to assist professional therapists. Significant improvements have been reported in certain areas of human robot rehabilitation research. Research on human robot interaction (HRI) is still new and immature compared to works on human expression 'mimicking', where the latter is crucial especially for rehabilitation. Engagement is an important element for HRI which is still lacking due the complex process involve in acquiring the accurate measurement of human affective state. At the moment, only invasive and contact procedures of physiological parameters of sympathetic nervous system activity have been used. While engagement is an important process for HRI and real-time information is needed, the current methods are unsuitable and cause discomfort as well as awkwardness during the rehabilitation process. Therefore, in the case of subjects with special needs, the sensors use should be portable to allow mobility while not hindering with patient monitoring, communication or even life support system [3].

Human behaviours are affected by several factors; genetics, social norms, faith and attitude. Some behaviours are deemed to be acceptable while others are not. In most cases, human behaviours can be best expressed through emotional reactions to external stimuli. These can be manifested through speech, facial expressions, body languages and physiological signals (EEG, heart rate, blood flow, Galvanic Skin Response (GSR), etc.). Over the last two decades, progress has been made in affective computing using the Autonomic Nervous System (ANS) parameters for affect detection. Yet, while a significant number of findings have been reported, most of these experimentations used invasive approaches where direct contact between subject and sensor was required. The maturity and evolution of sensing technique have made contact-less and non-invasive ANS responses monitoring possible through the application of thermal imaging which has shown a potential in characterising the subdivision of ANS [4].

Over the years, several studies have showed the exploitability of facial skin temperature for affective states recognition. Merla states that "Measuring subtle thermal effect due to emotional arousal may provide useful information about the sympathetic activity" [4]. In most existing researches, there are two ways for extraction of features from the thermal images; imaging features and temperature features [5]. Here are some of the literatures that extracted imaging features from the imaging feature: Yasunari Yoshitomi et al. (2010) extracted the features by using a two-dimensional discrete cosine transformation (2D-DCT) to transform the gray scale values in the facial area into frequency components, and later used these extracted features in the expression recognition systems [6]. Benjam´ın Hern´andez, Gustavo Olague et al. (2007) had chosen the Gray Level Co-occurrence Matrix (GLCM) for region descriptors computation of the infrared images based on second order statistics features to distinguish the expressions of surprise, happiness and anger [7]. From the temperature features; Masood Mehmood Khan et al. (2009) have exploited the variances in the thermal intensity values recorded at thermally significant locations on human faces as the features to distinguish pretended and evoked emotional expressions [8]. Brain R. Nhan and Tom Chau have extracted the time, frequency and time-frequency features derived thermal infrared data to classify the natural responses of subject- levels of arousal and valence induced by the International Affective Picture System (IAPS) and others as mentioned in [3].

The remaining part of this paper is organized as follows: Section 2 presents the Experimental Design (Stimuli, Induced Emotion and Data Collection). Section 3 describes some processes require for in the affect detection from thermal image (Thermal Image Acquisition, Pre-processing & ROIs Generation, Feature Extraction and Classification). Lastly, Section 4 describes on the finding and discussion.

II. EXPERIMENTAL DESIGN

The setup for the experiment is illustrated in **Figure 1**. The data collection process was conducted in a confined room where the relative humidity and temperature were maintained at 50% and 24℃ throughout the session. The subject seating and thermal camera placements are illustrated in **Figure 1**. The facial thermal infrared data were captured using FLIR T420 (**Figure 2**) long-wave infrared (LWIR) and streamed through USB connection to the computer. The T420 thermal camera operated between 7.5 to 13 micrometres spectral ranges with thermal sensitivity (N.E.T.D) of < 0.045 ℃ at 30 ℃. The N.E.T.D. which stands for noise equivalent temperature difference measures the detector sensitivity. The resolution of the camera is 320 x 240 pixels (76,800 pixels). To capture the frontal face of the subject, the thermal camera was placed at eye-level roughly one meter from the subject. The thermal image data were streamed to the computer of 30 frames per second (fps) and saved in video format. The internal parameters of the T420 such as emissivity constant, measured distance, relative humidity and atmospheric temperature were set accordingly. The commonly agreed value for human skin emissivity constant of 0.98 was chosen. A total of 10 subjects were recruited comprising of 5 males and 5 females aged between 21 to 28 years old (mean age: 23 years old). The subjects were reminded not to consume any vasomotor substances (caffeine, nicotine etc.) and drugs prior to data collection day. In addition, they were also recommended to have their lunch or any heavy meals at least one hour before the data collection to avoid the metabolic effect of digestion. The data collection process consisted of two stages; emotion elicitation and self-report. The data collection process took place at a specific time of the day, for instance, 10 a.m. to 12 p.m. and 2 p.m. to 4 p.m. This allotted time was observed to standardise the data quality and minimise the effect of the circadian rhythm [9].

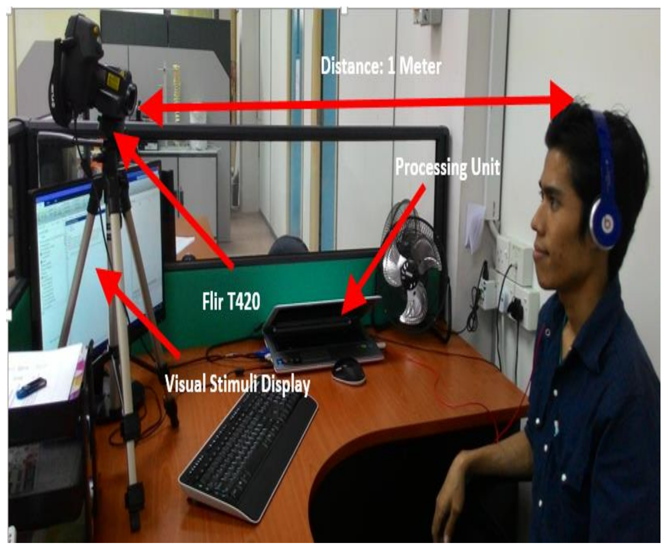

Figure 1 Setup for Data Collection

A. Stimuli

For the purpose of emotion elicitation, a specific video clips had been administered to the subjects through the monitor. The video clips were chosen because of the sound and music contribution to emotion elicitation as being reported in several studies [10, 11]. Common methods for stimulating affective states include affective picture viewing [3], movie clips [4], startle auditory [12], Stroop Color Word Conflict Test [13], and Mock crime scenario based questions [14,15] etc. The duration of the selected audio-visual stimuli spanned between two to four minutes. The lists of stimulants selected and its corresponding emotions are tabulated in **TABLE I.**

TABLE I STIMULANT AND ITS SOURCE

Emotion	Stimulant (Source: Video)
Happy	Just for Laughs Gags: Turning Wine into Spit
Sad	Newest88: A Father's Love for His Daughter
Fear	Movie clips: Saw 3- The Rack (2006)

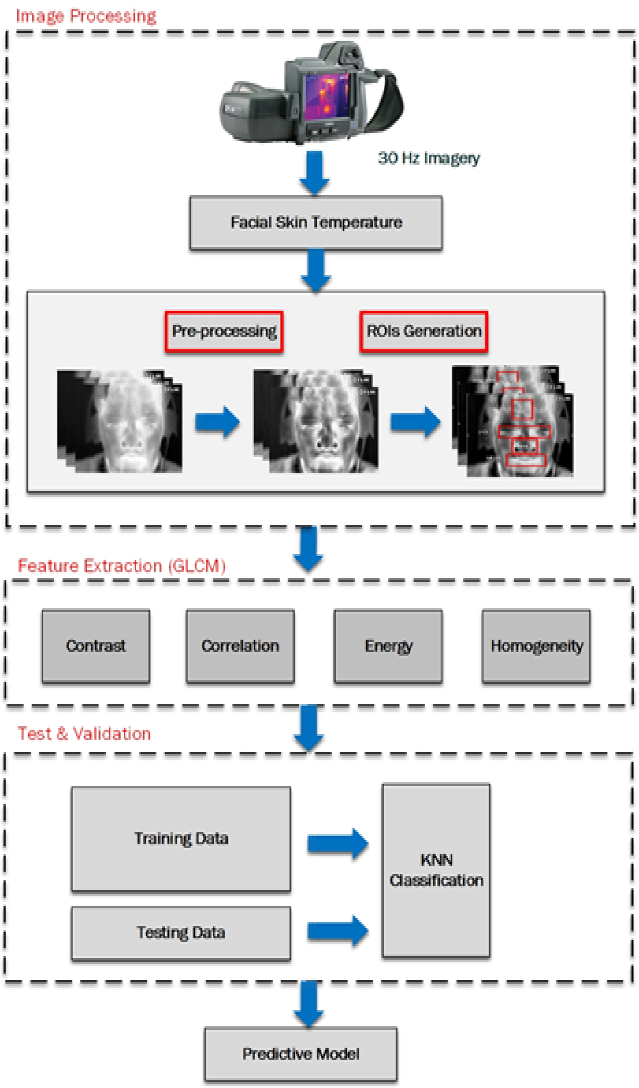

Figure 2 Proposed framework

B. *Induced Emotion*

In our experiment, three basic human emotions have been tested named as Happy, Sad and Fear. The selection of these emotions was based on the fact that it was completely opposite to one another.

C. *Data Collection*

The proposed framework adopted in our experiment is shown in **Figure 2**. The framework consists of three main blocks; Image Processing, Feature Extraction and Test & Validation. In the first block, Image Processing: the steps involved include image acquisition (30 fps), pre-processing and ROIs generation. The second block is the feature extraction. In this experiment, we used the GLCM based feature extraction to extract second order statistic from the thermal images. The features obtained from the thermal images were Contrast, Correlation, Energy and Homogeneity. Next, the last block is the test and validation. In this stage, we used the 10-fold cross validation for validation purposes with k-Nearest Neighbor (KNN) Classifier.

III. AFFECT DETECTION FROM THERMAL IMAGES

This section discussed the steps involved in the implementation of thermal image for affect detection. The details are provided as follows.

A. *Thermal Image Acquisition*

The acquisition of thermal images was done in a controlled room with relative humidity of 50%, 24 ℃ and uniform illumination. The subject is seated 1.0 meter from the thermal camera (refer **Figure 1**- Setup for Data Collection) and advice to maintain minimum head movement. The camera's framerate for data collection was set at 30 frames per second (fps). For one set of video, there are 1200 images being captured. The dataset was then down sampled to 80 images per subject for each emotion. This step was done to minimize the computational cost (memory and time). The image samples are showed in **Figure 3**.

Figure 3 Images sample (radiometric)

B. *Pre-processing and Region of Interests Segmentation*

Figure 4 shows the pre-processing sequences and the Region of Interests (ROIs) segmentation stage that take part in the Image Processing block. The raw images were normalized using contrast limited adaptive histogram equalization (CLAHE) [16]. The CLAHE algorithm works by applying the histogram equalisation to each equal size non-overlapping sub-regions. For a thermal image *I*, let the *M* be the numbers of pixels and *N* be the grayscales in each region. Then, let the histogram value at location (*i, j*) be defined as $h_{i,j}(n)$, where $n = 0, 1, 2,\ldots, N\text{-}1$. Hence, the estimate for the corresponding cumulative density function (CDF) scale by (*N-1*) can be expressed as shown in (1).

$$I_{i,j}(n) = \frac{(N-1)}{M} x \sum_{k=0}^{n} h_{i,j}(k) \quad (1)$$

The result from (1) is referred as the histogram equalisation. However, this method causes the region contrast to upsurge to the maximum value. This can be treated by introducing a clip limit denoted by β which limits the slope of (1) to the desired level. The clip factor, denoted by α is controlling the clip limit. The value of α was represented in percent. The clip limit β is defined as:

$$\beta = \frac{M}{N}\left(1 + \frac{\alpha}{100}(S_{max} - 1)\right) \quad (2)$$

The S_{max} is the maximum allowable slope yielded when the clipping factor α equal to hundred percent. The recommended value of S_{max} is four for still X-ray images, however, for other applications the value of S_{max} need to be determined by trial and error. As the clip factor α increases from zero to hundred, the value of S_{max} is changing within the range of one to S_{max}. The value of clip limit β was set to be 0.01 in our experiment. There are three types of distribution options available in CLAHE algorithm implementation; Uniform, Rayleigh and Exponential. The range of clip limit is limited between zeros to one in the implementation. The higher number of this clip limit will result in higher contrast level. **Figure 5** depicts the comparison between raw image and contrast adjusted image.

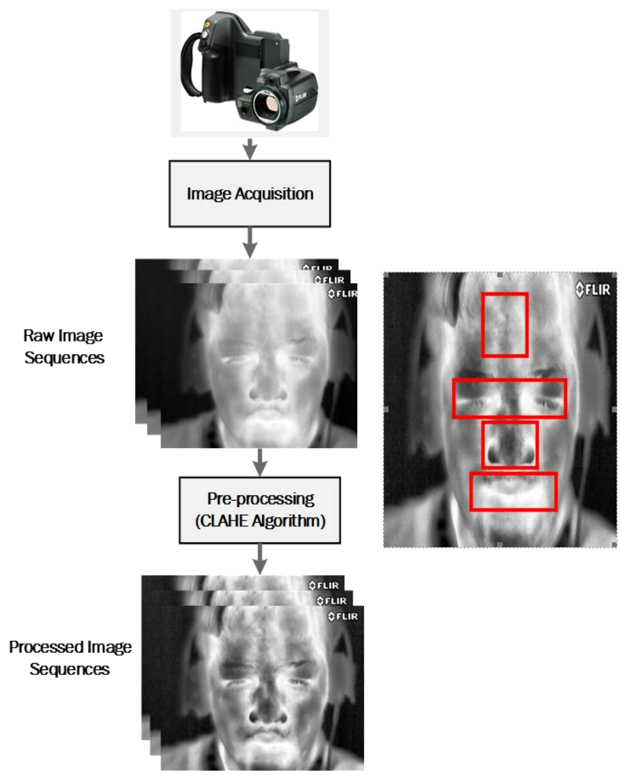

Figure 4 Pre-processing sequence & ROIs segmentation

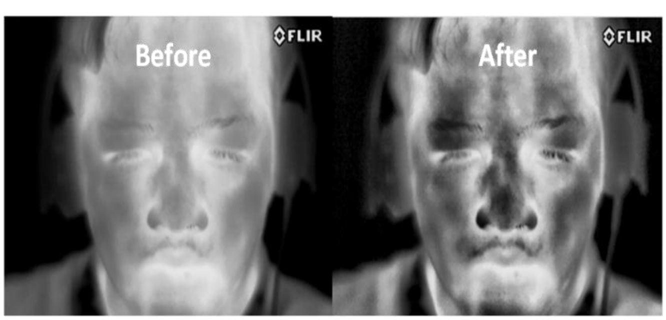

Figure 5 Comparison between raw and processed image

The Region of Interests (ROIs) segmentation was accomplished by specifying the location of the bounding box. For each emotion, four ROIs were segmented from the thermal image of the face. These ROIs were periorbital, supraorbital, mouth and nose.

C. Feature Extraction

For the feature extraction, a widely used texture based feature extraction known as Gray Level Co-occurrence Matrix (GLCM) has been chosen. The GLCM characterize second order statistic of an image by computing how often pairs of pixel with specific values and in a specified spatial relationship occur in an image. The features are generated by calculating the features for each one of the co-occurrence matrices obtained by using the directions 0°, 45°, 90°, and 135° and specific displacement distances. For the computation of GLCM, we used four displacement distances, d = 1, 2, 3 and 4 and four orientations, θ = 0°, 45°, 90°, and 135° (illustrated in **Figure 6**). For each element (i, j), in the resultant GLCM is simply the sum of the number of times that the pixel with value i occurred in the specified spatial relationship to a pixel with value j in the input image, $P_{i,j}$. The GLCM is a matrix where the number of rows and columns are equal to the number of grey levels, denoted by G. The element of the matrix $P(i, j \mid \Delta x, \Delta y)$ is known as the relative frequency separated by a pixel distance $(\Delta x, \Delta y)$. The probability (P_R) can be defined can be defined as in (3) [17].

$$P_R(x) = \{C_{i,j} \mid d, \theta\} \tag{3}$$

The number of grey level occurrences in row (i) and column (j) is represented by variable $C_{i,j}$.

$$C_{i,j} = \frac{P_{i,j}}{\sum_{i,j=0}^{G-1} P_{i,j}} \tag{4}$$

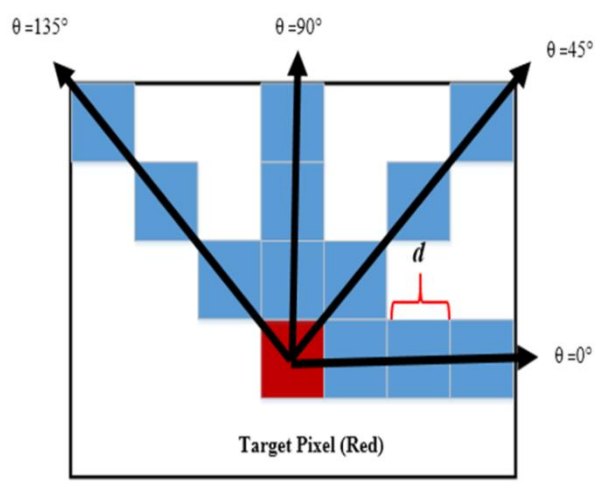

Figure 6 Comparison between raw and processed image

There are fourteen statistical features that can be extracted from GLCM. However, only four most used statistical features were considered (contrast, correlation, energy and homogeneity) to reduce the complexity of the dataset. Table 2 elucidates the offset representation.

TABLE II OFFSET REPRESENTATION FOR INTERPIXEL DISTANCE, D=1,2,3,4 AND ORIENTATION, Θ= 0°, 45°, 90°, 135°

Orientation	Offset	
0°	0	1
	0	2
	0	3
	0	4
45°	-1	1
	-2	2
	-3	3
	-4	4
90°	-1	0
	-2	0
	-3	0
	-4	0
135°	-1	-1
	-2	-2
	-3	-3
	-4	-4

Hence, for each ROI, there are (64 features x 80 images = 5120 features vector) per subject. For 10 subjects, a total of 51200 features vector were obtained for each emotion. The resultant dataset for three emotions (Fear, Happy and Sad) were 153600 features vector. The dataset (EmotionData) then represented in the form of 153600 features x 4 ROIs (Periorbital, Supraorbital, Mouth and Nasal).

D. Classsification

In this experiment, we had tested k-Nearest Neighbor (k-NN) classifier and Tree classifier for the classification of three basic emotions (Fear, Happy and Sad). The classification process was performed using the Classification Learner in Matlab 2015a. The dataset, EmotionData, 153600 x 4 features of size were fed into the classifier. The ROIs served as the predictor while the EmotionLable served as the response of the classifier. Besides, the 10-fold cross validation was selected for the model validation. There are three options available for model validation in Classification Learner; k-fold cross validation, holdout and no validation.

For the k-NN classification, the optimum value of neighbor (k) was determined based on the cross-validation method. By listing the probable values of k spanning from 1 to 153600, a set of logarithmically spaced vector were obtained. These values were then selected as the number of nearest neighbor while looping through 10-fold cross-validation scheme. The performance of the classification based on the selected neighbor is depicted in **Figure 7**. The selection of optimum neighbor is of upmost important because the k-NN classifier is sensitive to the selection of neighbor (k). Small value of k resulted in noise sensitive model while large value of k significantly reduced the model accuracy. The working principal of k-NN can be summarized as follows:

Input: ***M***, the set of k training objects, the test object

v= (x', y')

Step:

Measure the distance ***d (x', x)*** between ***v*** with every object in feature space, **(x, y) ∈ *M*.** Then, select $M_v \subseteq$ **M,** the set of k-closest training to ***v***

Output: $y' = \arg\max_z \sum_{(x_i, y_i) \in M_v} w_i \times I(z = y_i)$

where the distance, $w_i = \dfrac{1}{d(x_q - x_i)^2}$; x_q is the query point and x_i is the reference point.

The function $I(.)$ returns 1 if true and 0 otherwise. The class label is *z* and the y_i is the label of the i^th nearest neighbours.

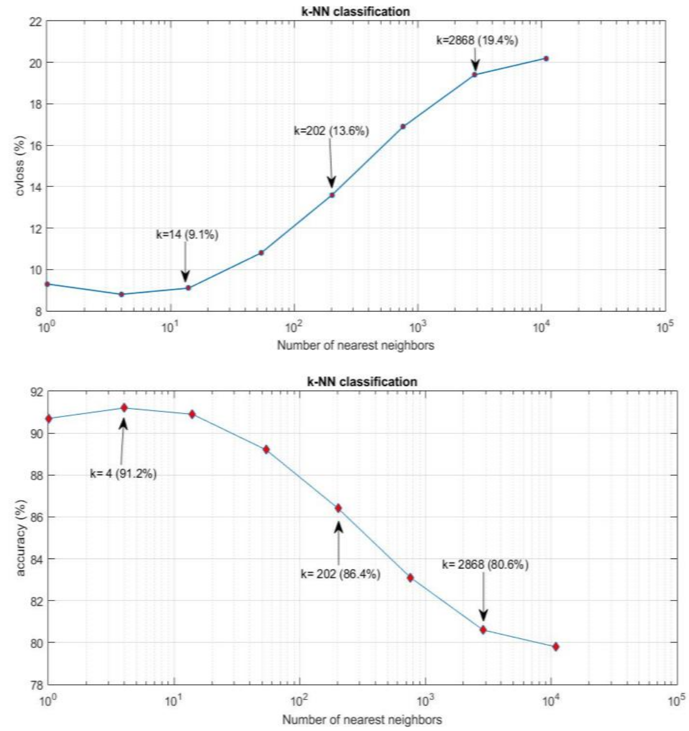

Figure 7 Selection of neighbor (k)

IV. RESULT AND DISCUSSION

Figure 8 shows the matrix of scatter plot by group plotted using *gplotmatrix* function to display an array of all the bivariate scatterplots between our 4 variables, along with a univariate histogram for each variable. The points in each scatterplot are color-coded by the emotion label; Cyan for Happy, Magenta for Sad and Blue for Fear. This scatter plot was used to view the lower dimensional subspace of the dataset. As mentioned in previous section, in this experiment we tested several classification techniques to get the best classification result for the three basic emotions; Fear, Happy and Sad. Table 3 shows the comparison for the classifier performance. For the weighted k-NN, the Euclidean distance metric was used and the distance weight was set as squared inverse of the Euclidean distance. The number of neighbours for the weighted k-NN was varied from 5 to 50 to observe the changes in terms of overall accuracy.

TABLE III CLASSIFIER PERFORMANCE COMPARISON

Classification Method	Feature	Accuracy (%)
Tree Complex	GLCM	33.9
Tree: Medium	GLCM	36.9
KNN: Fine KNN	GLCM	90.7
KNN: Weighted KNN (k=5)	GLCM	91.2
KNN: Weighted KNN (k=10)	GLCM	91.1
KNN: Weighted KNN (k=30)	GLCM	90.1
KNN: Weighted KNN (k=50)	GLCM	89.4

The k-NN classifier is sensitive to the selection of the neighbor (k). This can be observed from **Figure 7** which depicted the model accuracy versus the number of neighbors. The tradeoff between the accuracy and the noise rejection need to be considered carefully. Henceforth, as a means to strike a balance, the value of k (k=30) was chosen and conjectured ample for the weighted majority voting to assign the appropriate class label.

The highest classification accuracy was showed by the Weighted k-NN (k=5) with 91.2% overall accuracy and followed by Fine k-NN with 90.7% overall accuracy. **Figure 9** elucidates the confusion matrix for the Weighted k-NN (k=30). From the confusion matrix, important parameters such as True Positive (TP), True Negative (TN), False Positive (FP), False Negative (FN), True Positive Rate (TPV), False Negative Rate (FNR), Positive Predictive Rate (PPR), and False Discovery Rate (FDR) could be extracted for performance evaluation.

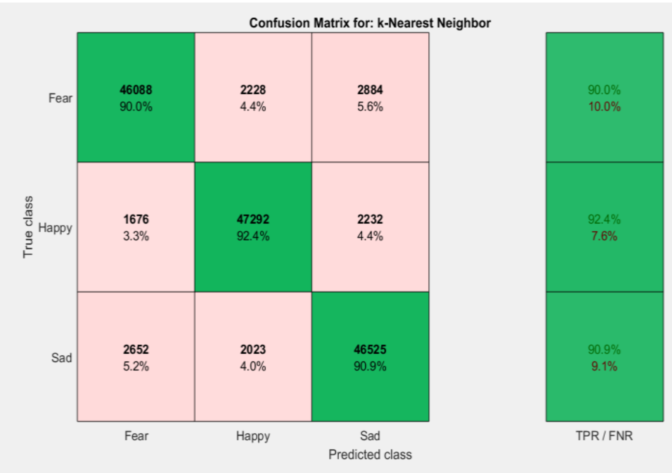

Figure 9 Weighted k-NN (k=30) confusion matrix

Table 4 shows the detail accuracy by class of emotions for the Weighted k-NN (k=30) classifier. There are five performance components could be observed from the table; True Positive (TP), False Positive (FP), Precision, Recall and F-Score. The performance scores were slightly different from the one provided by the confusion matrix because of the difference computational approach (confusion matrix was computed using Matlab while the detail accuracy by class of emotion was computed in WEKA.

TABLE IV DETAIL ACCURACY BY CLASS (WEIGHTED K-NN)

TP Rate	FP Rate	Precision	Recall	F-Score	Class
0916	0.043	0.913	0.916	0.915	**Happy**
0.897	0.054	0.893	0.897	0.895	**Sad**
0.897	0.048	0.903	0.897	0.90	**Fear**
0.903	**0.048**	**0.903**	**0.903**	**0.903**	**Weighted Average**

The overall accuracy recorded was around 90.3%. The k-fold loss from the 10-fold cross validation was around 9.7%. The Happy class shows the highest true positive (TP) rate as compared to the rest of the classes in the range of 91.6%. On the contrary, both the Fear and Sad class shared the same value for the true positive (TP) rate. It can be observed that the Sad class recorded the highest false positive (FP) rate which indicates that it is most likely produce more negative prediction as compared to positive prediction. In terms of Precision, Recall and F-Score, the Happy class outperformed the remaining two classes of emotion. It is impractical to benchmark this model against other existing models due to the disparities in terms of emotions tested, the number of subjects, thermal camera resolutions, region of interests (ROIs) selection and so forth. The performance comparison and benchmarking with others approach for the time being is unreasonable unless same dataset is utilized.

In this experiment, we attempted to classified different emotional states from the thermal imaging by using texture based feature extraction, GLCM. From the result, the overall accuracy of the predictive model developed using k-NN had shown good accuracy in the range of 90.1%. With the small resulted k-fold loss, we are positive and optimistic that the predictive model would perform well in real life scenario. By considering several features extraction methods, the overall performance might be improved due to availability of several distinct features. The known limitation for thermal imaging based affect detection as stated from a few studies is the environmental condition plays the crucial role as the homeostasis and the cutaneous temperature are continuously regulated. In order to avoid attributing any psychological valence to unmitigated thermoregulatory, proper countermeasures and cautions should be adopted. Our research is far from being conclusive. However, these findings are utmost promising.

ACKNOWLEDGMENT

We wish to express our gratitude to the Ministry of Higher Education (MOHE) for funding the project under the Fundamental Research Grant Scheme (FRGS), Grant no: FRGS13-076-0317. Our deepest appreciation also goes to postgraduate student and lecturers involved in making this project possible.

REFERENCES

[1] W. R. Picard, "Affective computing: challenges," International Journal of Human-Computer Studies - Application of affective computing in human—Computer interaction, vol. 59, pp. 55-64, 2003

[2] M.Berking & B. Whitley, "Emotion Regulation: Definition and Relevance for Mental Health", in M. Berking & B. Whitley (Eds.), Affect Regulation Training: A Practitioners' Manual. New York: Springer, pp. 5-17, 2014. CrossRef

[3] B. R. Nhan and T. Chau, "Classifying Affective States Using Thermal Infrared Imaging of the Human Face," IEEE Trans. Biomedical Eng., vol. 57,no. 4, pp. 979-987, April 2010. CrossRef

[4] A. Merla and G.L. Romani, "Thermal signature of emotional arousal: a functional infrared imaging study," Proceedings of the 29th Annual International Conference of the IEEE EMBS Cite Internationale, Lyon, France, August 23-26, 2007. CrossRef

[5] L. Zhilei and W. Shangfei."Emotion Recognition using Hidden Markov Models from Facial Temperature Sequences," Springer-Verlag Berlin Heidelberg, pp. 240-247, 2011.

[6] Yoshitomi, Y. "Facial Expression Recognition for Speaker Using Thermal Image Processing and Speech Recognition System," in Proc. of 10th WSEAS International Conference on Applied Computer Science, pp. 182–186, 2010.

[7] B. Hern´andez,G. Olague, R. Hammoud, L. Trujillo,E. Romero." Visual learning of texture descriptors for facial expression recognition in thermal imagery." in Computer Vision and Image Understanding 106(2-3), pp. 258–269, 2007.

[8] M.M. Khan, R.D. Ward and M. Ingleby . "Classifying pretended and evoked facial expressions of positive and negative affective states using infrared measurement of skin temperature," Trans. Appl. Percept. 6, 1, 2009. CrossRef

[9] K.Krauchi & A. Wirz-Justice, "Circadian rhythm of heat production, heart rate and skin and core temperature under unmasking condition", in men. American Journal of Physiology, 267 (3), pp. 819-829, 1994.

[10] M. Murugappan & S. Murugappan, "Human emotion recognition through short time Electroencephalogram (EEG) signals using Fast Fourier Transform (FFT)", in Signal Processing and its Applications (CSPA), 2013 IEEE 9th International Colloquium, 2013. CrossRef

[11] Murugappan, M., & Murugappan, S. (2013). Human emotion recognition through short time Electroencephalogram (EEG) signals using Fast Fourier Transform (FFT). Paper presented at the Signal Processing and its Applications (CSPA), 2013 IEEE 9th International Colloquium. CrossRef

[12] M.Wollmer,F.Weninger,T. Knaup, B. Schuller, C. Sun, K. Sagae, & L-P. Morency,"YouTube Movie Reviews: Sentiment Analysis in an Audio-Visual Context", in Intelligent Systems, IEEE, 28(3), pp. 46-53, 2013. CrossRef

[13] D. Shastri, A.Merla, P. Tsiamyrtzis, and I. Pavlidis, "Imaging facial signs of neurophysiological responses," IEEE Trans. Biomed. Eng., vol. 56, no. 2, pp. 477–484, Feb. 2009. CrossRef

[14] I. Pavlidis, J. Dowdall, N. Sun, C. Puri, J. Fei, andM. Garbey, "Interacting with human physiology," Comput. Vis. Image Understanding, vol. 108, no. 1–2, pp. 150–170, 2007. CrossRef

[15] I. Pavlidis and J. Levine, "Thermal image analysis for polygraph testing," IEEE Engineering in Medicine and Biology Magazine, 21(6):56 – 64, 2002. CrossRef

[16] Z. Zhu, P. Tsiamyrtzis and I.Pavlidis, "Forehead thermal signature extraction in Lie Detection,"in Proceeding of the 29th Annual International Conference of the IEEE EMBS Cite Internationale, Lyon, France, August 23-26, pp.243-246, 2007. CrossRef

[17] T. Bourlai, A.Ross, C.Chen and L.Hornak " A Study on Using Mid-Wave Infrared Images for Face Recognition," in Sensing Technologies for Global Health, Military Medicine, Disaster Response, and Environmental Monitoring II; and Biometric Technology for Human Identification IX, Proc. of SPIE Vol. 8371, 2012. CrossRef